Received: 1 July 2022 | Revised: 14 December 2022 | Accepted: 22 December 2022

DOI: 10.1111/vop.13057

ORIGINAL REPORT

WILEY

Morphology and volume of Meibomian glands ex vivo pre and post partial tarsal plate excision, cryotherapy and laser therapy in the dog using microCT

Victoria Zwiauer-Wolfbeisser[1] | **Stephan Handschuh**[2] | **Alexander Tichy**[3] | **Barbara Nell**[1]

[1]Department of Companion Animals and Horses, University of Veterinary Medicine, Vienna, Austria

[2]VetCore Facility for Research, University of Veterinary Medicine, Vienna, Austria

[3]Department of Biomedical Sciences, University of Veterinary Medicine, Vienna, Austria

Correspondence
Victoria Zwiauer-Wolfbeisser, Small Animal Surgery, Ophthalmology Service, Veterinary University of Vienna, Veterinaerplatz 1, Vienna A-1210, Austria.
Email: victoria.zwiauer@vetmeduni.ac.at

Abstract

Objective: To determine the morphology and volume of Meibomian glands (MG) of dogs with microCT before and after partial tarsal plate excision (PTPE), cryotherapy, and laser therapy.

Procedure: MicroCT scans were made of 12 upper lids (ULs) and lower lids (LLs) of 12 dogs. After undergoing PTPE, 10 ULs and LLs were scanned again, and one UL and one LL was scanned after laser therapy and one UL and one LL after cryotherapy.

Results: The length of the area containing MGs did not change pre- and post-PTPE, and cryo- or laser therapy. The mean number of MGs in the ULs and LLs was 30.50 and 29.42, respectively, and did not change during the procedures. The average length of one individual MG was 2.60 mm. The mean volume of MGs in the 10 ULs and LLs pre-PTPE was 21.45 and 17.2 mm^3, respectively, and 12.84 and 11.25 mm^3 in the UL and LL after PTPE, respectively. The mean volume of MGs decreased from 29.78 mm^3 precryotherapy to 28.91 mm^3 post-treatment and in the lower eyelid from 22.87 to 22.4 mm^3 after cryotherapy. The mean volume of MGs in the UL and LL before laser therapy was 8.95 and 6.78 mm^3, respectively, and after 9.25 and 6.38 mm^3, respectively.

Conclusion: MicroCT is a valuable tool to determine the morphology and the volume of MGs and to demonstrate changes that occur after PTPE, laser-, and cryotherapy. There is no need for additional preparation, such as staining, of the specimen prior to scanning.

KEYWORDS

cryotherapy, dogs, laser therapy, Meibomian glands, microCT, partial tarsal plate excision

1 | INTRODUCTION

The Meibomian glands (MGs) are one of the most important glands of the eye. Located alongside the glands of Zeis, the MGs are essential for the production of the outer layer of the tear film, the lipid layer. They play an important role in the stabilization of the tear film after blinking.[1]

Occasionally, hair follicles are located in the MG, resulting in Distichiasis. Distichiasis (di- = two, stichio = row) is the presence of aberrant, lash-like hairs along the free edge of the lid.[2] The hair follicles of the distichia are either located next to the MGs or within the glands.[3] Hairs usually arise from the openings of the MGs, sometimes solitary, sometimes in tufts of two or more hairs. If the cilia are thick and bristly and grow toward the cornea, it can lead to blepharospasm, epiphora, superficial inflammation of the cornea (superficial keratitis), and even deep corneal ulcerations.[4] Distichiasis has been described in many different animals and in humans.[5] Removing the aberrant lash by plucking is not sufficient as a long-term treatment, but can be very helpful in identifying the distichiasis as the trigger of an irritation.[6] Destruction of the hair follicles is considered a long-term form of treatment for distichiasis. There are various options, including electro- or laser epilation, cryotherapy, and partial resection of the tarsal plate. During all of these procedures all parts of the eyelid, especially the MGs are heavily manipulated or even destroyed. The destruction or reduction in intact MGs could result in a clinical impact regarding the ocular surface. As the MGs are located alongside the glands of Zeis, the MGs are essential for the production of the outer layer of the tear film, the lipid layer. A destruction of MGs following cryotherapy, laser therapy, or PTPE as treatment for distichiasis, could therefore lead to pathologies regarding the composition of the precorneal tear film or even Meibomian gland dysfunction (MGD). The present study investigates the use of microscopic X-ray computed tomography (microCT) for studying the size and morphology of Meibomian glands in fresh eyelid biopsies. It was found that microCT allows visualization of Meibomian glands as well as measurement of Meibomian gland volume, requiring neither tissue fixation nor treatment with X-ray dense contrast agents. We identified the morphology and volume of the MGs before and after a partial tarsal plate excision as well as after cryotherapy or laser therapy. We hypothesize that a partial tarsal plate excision (PTPE) leads to a destruction and reduction in the number of intact MGs.

2 | MATERIAL AND METHODS

From January 2021 until August 2021, 12 upper lids (UL) and lower lids (LL) from 12 different dogs were collected. The 12 dogs were presented to the ophthalmology department of the University of Veterinary Medicine Vienna for enucleation due to various reasons. Of the 12 dogs, three were males, two were castrated males, one was female, and four were spayed females. The reason for enucleation included iris melanoma (two cases), glaucoma (three cases), and the remaining seven cases consisted of lens-induced uveitis, corneal abscess, corneal perforation, anterior lens luxation, descemetocele, and bulbar prolapse. There were four right eyes (OD) and eight left eyes (OS). The average age of the dogs at the time of enucleation was 8.25 years (range 3–12 years). The average weight of the 12 dogs was 16.9 kg (range 2.6–36 kg). One of the dogs (dog 5) suffered from keratoconjunctivitis sicca (KCS) on both eyes at the time of enucleation, with a Schirmer tear test 1 (STT-1) of 12 mm/min. Another dog (dog 10) had previously suffered from KCS on both eyes but had a normal STT-1 (>15 mm/min) before the enucleation. (Table 1).

One to 3 h after the operation, each of the lids was placed in a small plastic bag (PolyZip bag 120 x 170 mm with labeling field), wrapped in a sterile swab, and stored between 4°C and 7°C. In order to distinguish the UL from the LL, the UL was labeled with a single suture (Vicryl

TABLE 1 Signalment, reason for enucleation, treatment, and STT-1

Dog	Age (years)	Sex	Breed	Weight (kg)	OS/OD	Reason for enucleation	Treatment	STT-1 (mm/min)
1	12	Male castrated	Havanese	5.8	OS	Ablatio retinae	PTPE	>15
2	3	Male	Labrador Retriever	30.0	OS	Limbal melanoma	PTPE	>15
3	11	Female spayed	Boston Terrier	9.0	OS	Corneal abscess	PTPE	>15
4	11	Female	Mixed breed	22.0	OS	Iris melanoma	PTPE	>15
5	4	Female spayed	French Bulldog	10.6	OD	Corneal perforation	PTPE	12
6	12	Male	Mixed breed	22.7	OD	Iris melanoma	PTPE	>15
7	8	Male castrated	Mixed breed	14.5	OD	Glaucoma	PTPE	>15
8	7	Male	Tibetan Terrier	13.8	OS	Glaucoma	PTPE	Unknown
9	12	Female spayed	Mixed breed	23.5	OD	Luxatio lentis anterior	PTPE	>15
10	5	Female spayed	French Bulldog	12.1	OS	Descemetocele	PTPE	>15
11	8	Male	Mixed breed	36.0	OS	Glaucoma	Cryotherapy	>15
12	6	Male	Yorkshire Terrier	2.6	OS	Prolaps bulbi	Laser therapy	Unknown

Abbreviations: OD, right eye; OS, left eye; OU, both eyes; PTPE, partial tarsal plate excision; STT-1, Schirmer tear test 1.

5/0). Meanwhile, 1.5% low-melt agarose was melted in a small container and then cooled down to 30°C–40°C. Both the labeled UL and LL were carefully placed together in one Eppendorf tube. The Eppendorf tube was then filled with 1.5% low-melt agarose and placed into the freezer until the agarose hardened. The tube was mounted to the sample holder (lid of the Eppendorf tube facing downward) with double-sided adhesive tape and additionally wrapped and stabilized with parafilm.

All of the 12 ULs and LLs were scanned, for the first scan, with microCT without any manipulation (first scan).

After the first microCT scan, the sample was stored between 4°C and 7°C. The next day the UL and the LL were removed from the Eppendorf tube with forceps, and the agarose was carefully removed with swabs. After cleaning the lids, a transconjunctival PTPE was performed in 10 of the 12 ULs and LLs. The lids were mounted in chalazion forceps, with the conjunctival side of the lid facing up. Two longitudinal, parallel incisions were made with a fine scalpel (Aesculap® Safety Scalpel No. 11). The first incision was placed approximately 2 mm from the free lid margin and the second approximately 4.5 mm from the free lid margin along the whole length of the lids, creating a tarsoconjunctival strip, approximately 2.5 mm wide and 2 cm long (depending on the length of the eyelid). This tarsoconjunctival strip was removed using iris scissors. The tarsoconjunctival strips and the remaining tissue of the UL and LL were placed together in a new Eppendorf tube.

To differentiate between the excision of the UL (ULE) and the excision of the LL (LLE), two methods were used. For the first five samples, a pipette tip was cut into two pieces and was placed into the Eppendorf tube to separate the remaining UL and the ULE from the remaining LL and the LLE. When these samples were evaluated, bubbles were present, which then led to difficulties reconstructing the MGs. The seven remaining samples were placed in the Eppendorf tube in a specific order, to assign them correctly during the evaluation. The UL and the ULE were always placed in the upper area (the area closer to the lid of the Eppendorf tube), while the LL and the LLE were placed into the lower part of the Eppendorf tube. The localization of the tissue samples did not change during the microCT scans.

Two of the 12 samples did not undergo PTPE. The UL and LL of dog 11 were treated with cryotherapy. Both the UL and the LL were mounted to a stack of sterile swabs with needles, with the conjunctival side facing up. The probe of the cryotherapy device was placed on the conjunctiva about 2 mm from the free lid margin for 3 s at a probe temperature of minus 80°C. The entire length of the UL and LL was treated, taking care not to overlap the localizations. Two rounds were performed on both the UL and LL. Afterward, the eyelids were again embedded in Eppendorf tubes filled with agarose.

The UL and LL of dog 12 were treated with laser therapy. Both the UL and the LL were again mounted to a stack of sterile swabs, with the conjunctival side of the lid facing up. The FOX 810 Ophthalmology Laser (A.R.C. Laser GmbH, 90411) was equipped with the distichiasis probe. The probe was inserted into every second MG opening of both eyelids. Treatment consisted of 2 cycles at 700 mW for 1.5 s each. After performing laser therapy, both eyelids were placed in an Eppendorf tube filled with agarose and taken to the second microCT scan.

All 12 samples and their excisions were scanned for a second time in the microCT after the respective treatment (second scan).

MicroCT was performed with the XRadia MicroXCT 400 (Carl Zeiss X-Ray Microscopy). The X-Ray settings were 40 kVp and 200 μA, and an additional X-Ray filter was used (Zeiss LE#1). A total of 1600 projection images were taken with a 0.4x detector; the exposure time was 10 s. The angular steps were 0.25°. The tomographic sections were reconstructed using XMReconstructer Software. The isotropic voxel size for each scan was 14.86 μm. The files were saved in a *.txm format.

The *.txm files were imported into the 3D visualization and analysis software Amira 2021.1® (FEI SAS, a part of Thermo Fisher Scientific). Three subsequent steps of image filtering were applied to reduce image noise. First, two 3D bilateral filters (Kernel Size X (px): 3, Kernel Size Y (px): 3, Similarity 20000; Kernel Size X (px): 3, Kernel Size Y (px): 3, Similarity 40000) were applied, followed by a 3D Gaussian filter (Standard Deviation (px): 1;1;1; Kernel Size Factor 2). After saving the new file, the MGs were segmented using the Amira 3D Segmentation Editor. The magic wand tool was used to segment the Meibom glands, based on their lower X-ray attenuation compared with adjacent tissue components. After the image segmentation, the MGs were visualized in 3D and labeled as MGs of the LL and UL, according to the suture markings and the specific placement in the Eppendorf tube.

Polygon surfaces were generated based on the segmentation of MGs. Linear distance measurements were made using the Amira 3D measuring tool. The length of the area of the LL and UL that contained MGs was measured and the results documented in an Excel File.

The number of MGs was manually counted. Using the Material Statistics tool, the total volume of MGs of both the UL and LL was calculated from the segmentation file. The length of the individual MGs of all 12 ULs and LLs was measured. When possible, the excretion ducts were measured as well. The overall morphology of the MG area was analyzed in all 12 samples, and certain changes were noted. These changes concerned shortening and dropout of individual MGs. All 12 samples were classified into four grades of shortening and dropout of MGs, according to a previously published grading scheme[7] (Table 2).

TABLE 2 Grading of shortening and dropout of MGs, according to Arita et al.[7] (MG: Meibomian gland)

Grade	Definition
Grade 0	No shortening or dropout of MGs in the total MG area
Grade 1	Shortening or dropout of less than one third of the total MG area
Grade 2	Shortening or dropout between one third and two thirds of the total MG area
Grade 3	Shortening or dropout of more than two thirds of the total MG area

With the Amira 3D program, the volume of the total MGs of both the UL and LL was calculated using the material statistics application. The data were then exported in an Excel format.

Following the second set of scans, the excision of the PTPE and the remaining tissue of the ULs and LLs were visualized using the 3D visualization. In all of the 10 samples that underwent PTPE, the excision margins went through the MGs, showing remnants of MG tissue in the excision and in the remaining tissue of the ULs and LLs.

The volume of the MGs in the excision and the remaining parts of the LL and UL was calculated and the data exported into an Excel format. For the LL and UL that were treated with cryotherapy and laser therapy, the same calculations were performed. The data were exported into an Excel format.

2.1 | Statistical analysis

Excel spreadsheets were used for statistical calculations. The statistical software, IBM SPSS Statistics 27, was used to calculate correlations. The probability was calculated between the grade of shortening and dropout and the age of the dogs using logistic regression. Values of $p < .05$ were considered significant.

3 | RESULTS

3.1 | Results of the first scan

The length of the area containing MGs ranged from a minimum of 1.90 cm to a maximum of 2.84 cm and a minimum of 2.00 cm to a maximum of 2.64 cm for the ULs and LLs, respectively. The length of the area containing MGs in the UL and LL did correlate negatively with age (correlation coefficient (r) −.458 and −.113, respectively) and positively with weight (r .344); however, those values were not significant (p-value > .05).

The mean number of MGs in the ULs was 30.50 (standard deviation (SD) = 2.71), and the median was 31 glands (range 26– 35). An average number of 29.42 (SD = 2.47) MGs was found in the LLs, with a median of 30 glands (range 26–35; Figure 1). The total number of MGs in the UL and LL combined correlated negatively with age (correlation coefficient (r) −.016) and positively with weight (r .043); however, both values were not significant (p-value > .05).

In the area closer to the free lid margin, the MGs were positioned parallel to each other and vertically to the tarsal plate. In the more proximal part of the lid, further from the free lid margin, the glands were no longer parallel but were bent in various directions in all samples. (Figure 2A) One dog (Dog 6) showed crisscrossing of the MG ends. (Figure 2B) In three dogs (Dog 5, 10 and 12), the ends of the MGs branched out into multiple endings. (Figure 2C).

The average length of one individual MG was 2.60 mm (SD = 0.66 mm), with a median of 2.65 mm (range 0.29–4.26 mm; Figure 3).

Excretion ducts were visible in all of the 12 samples, however not in every MG. The excretion ducts were localized more toward the conjunctival side of the free eyelid margin and angled in proximately 45° toward the conjunctival side, varying in length and shape. The majority of the MG ducts were shaped like a pyramid; however, some ducts were tube shaped. (Figure 2 arrows).

In all 12 ULs and LLs, it was possible to measure the lengths of 416 excretion ducts. The average length of the excretion duct of the MGs was 0.21 mm (SD = 0.08 mm), with a median of 0.20 mm (range 0.07–0.58 mm).

Four of the ULs (Dog 1, 4, 5, and 12) had no shortening of MGs (Grade 0). The LLs showed no shortening of MGs in two of the 12 samples (Dog 3, 5). Six (Dog 2, 3, 7, 9, 10, and 11) and 10 samples (Dog 1, 2, 4, 6, 7, 8, 9, 10, 11, and 12) showed an area of shortening less than one third of the total MG (Grade 1) area in the UL and LL, respectively. An area of shortening between one and two thirds of the total MG area (Grade 2) was detected in two (Dog 6, 8) of the ULs and none of the LLs samples. (Figure 4) Neither the ULs nor the LLs of the 12 samples showed an area of shortening more than two thirds of the entire MG area (Grade 3).

Four ULs (Dog 2, 6, 7, and 8) and one LL (Dog 10) showed a dropout area of less than one third of the total MGs (Grade 1) and eight ULs (Dog 1, 3, 4, 5, 9, 10, 11, and 12) and 11 LLs (Dog 1, 2, 3, 4, 5, 6, 7, 8, 9, 11, and 12) showed no dropout (Grade 0; Figures 4 and 5). A small but positive regression was found between the shortening of MGs and the age of the dogs, suggesting a higher risk of shortening with aging in both the UL and LL. The regression was not significant in the UL (regression coefficient

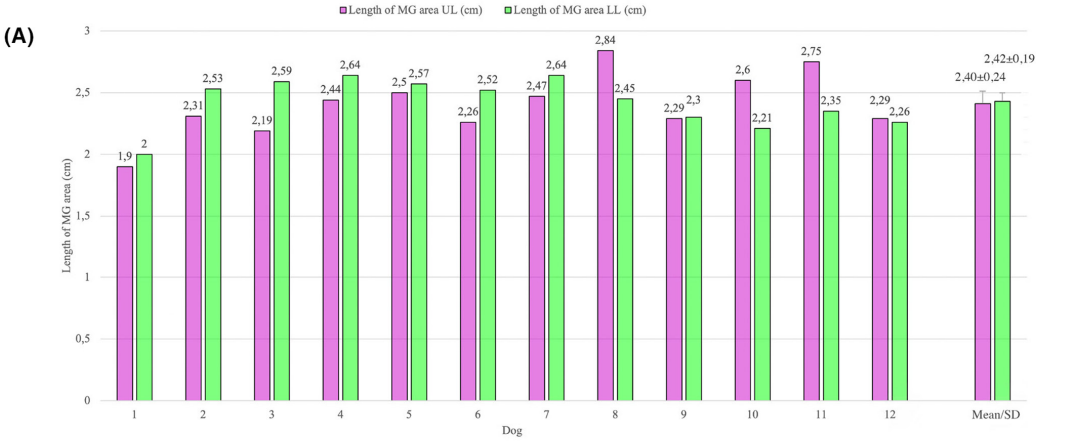

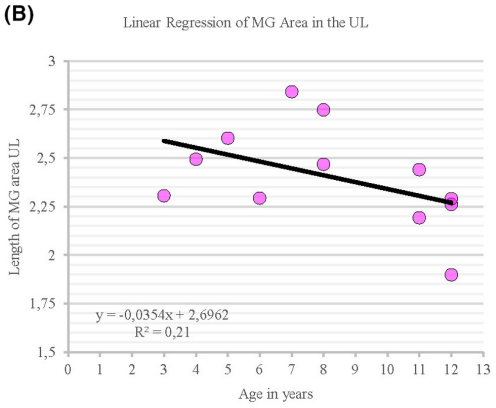

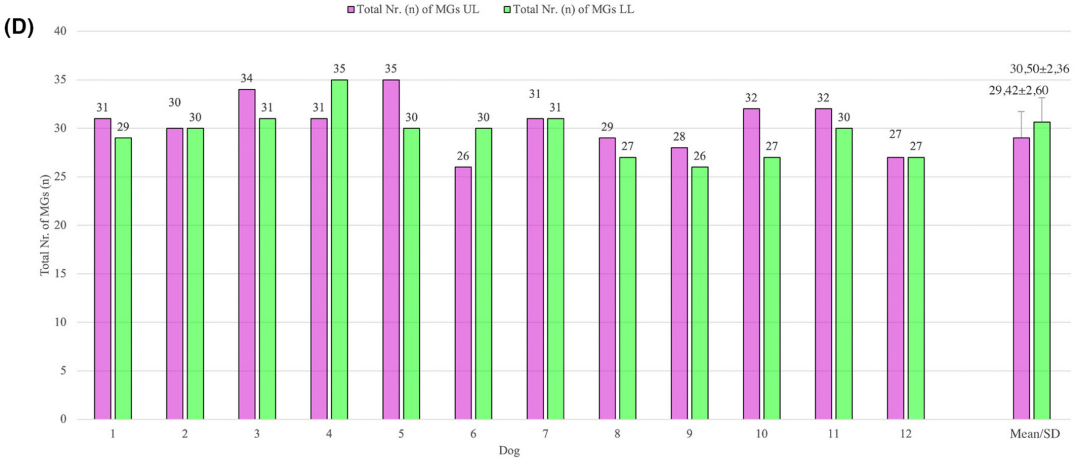

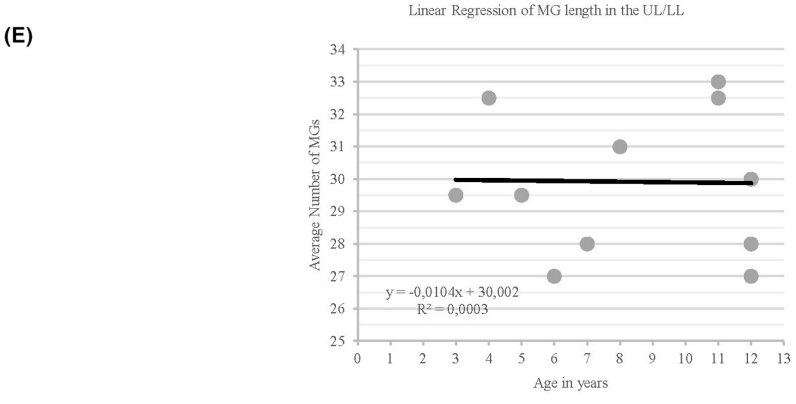

FIGURE 1 (A) Individual length of the area of the MGs in the UL and LL of each dog, mean length and SD of MG area of the UL and LL. (B) Linear regression model of the length of the area of MGs in the UL of the twelve dogs. (C) Linear regression model of the length of the area of MGs in the LL of the twelve dogs. (D) Individual number of MGs in the UL and LL of each dog, mean number of MG in the UL and LL as well as SD. (E) Linear regression model of the average number of MGs in the UL and LL and the age of the twelve dogs. MG, Meibomian gland; UL, upper lid; LL, lower lid; SD, standard deviation

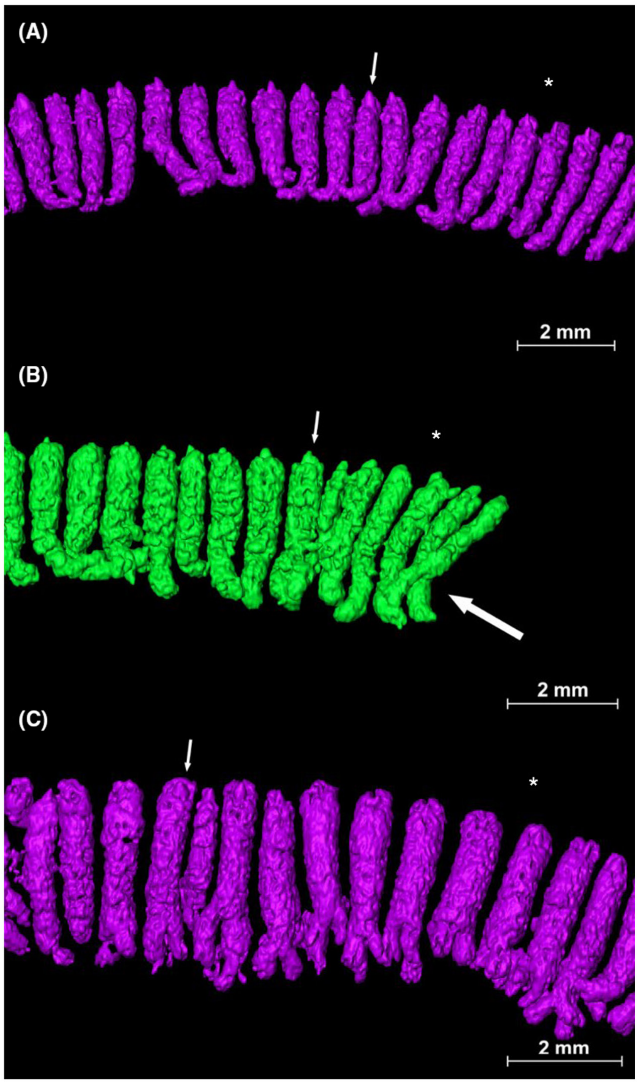

FIGURE 2 (A) Dog 4, 3D visualization of bending in MG endings in the UL (purple), with tube shaped excretion ducts (small arrow). (B) Dog 6, 3D visualization of criss-crossing (big white arrow) in MG endings in the LL (green), with pyramid shaped excretion ducts (small arrow). (C) Dog 5, 3D visualization of branching in MG endings in the UL (purple) with pyramid shaped excretion ducts (small arrow). The star (*) marks the position of the free lid margin. Isotropic voxel size = 14.8607 μm. MG, Meibomian gland; UL, upper lid; LL, lower lid

0.693, *p*-value .258), but significant in the LL (regression coefficient 1.609, *p*-value .038).

The regression model for the probability of age having an influence on the dropout grade of MGs was, both in the UL and LL, small but negative, suggesting that the risk of dropout in MGs went down with aging in both the UL and LL. The value for the UL was again not significant (*p*-value > .05), but was significant in the LL (*p*-value .022). Although a certain effect has been noted, these statistical calculations have to be regarded with care due to the small sample size.

The mean value of volume of the MGs of the 12 ULs was 21.45 mm^3, with a minimum of 8.95 mm^3 and a maximum of 41.72 mm^3. In the LL, the mean of the MGs volume was 17.2 mm^3, with a minimum value of 6.78 mm^3 and a maximum value of 23.18 mm^3. The average calculated volume of one MG in the ULs was 0.71 mm^3 and in the LLs 0.58 mm^3. There was a slight positive correlation between the average volume of MGs in the UL (*r* .367) and LL (*r* .563) and the weight of the dogs; however, both *p*-values were greater than .05 (.240 and .057, respectively). A positive correlation between the average volume of the MGs in the ULs and the number of MGs in the ULs was found (*r* .252), but not significant (*p*-value .429). However, the correlation between the volume of the MGs in the LLs and the number of MGs in the LLs was significantly positive (*r* .609; *p*-value .035). A positive correlation was also found between the length of the area in the ULs containing MGs and the volume of the MGs in the ULs, but not significant (*r* .049, *p*-value .879). On the contrary, the length of the area in the LLs did correlate significantly positive with the volume of the MGs in the LLs (*r* .732, *p*-value .007). The correlation between the length of the MGs area in ULs and the number of MGs in the ULs was positive but not significant (*r* .660, *p*-value .142). There was however a significant (*r* .632, *p*-value .028) positive correlation between the length of the MGs area in LLs and the number of MGs in the LLs.

3.2 | Results of the second scan after PTPE in dog 1–10

The area of MGs changed significantly after the PTPE procedure. The area was now separated into two parts: the tarsoconjunctival excision specimen and the remaining lid tissue. The amount of MGs did not change after PTPE. The length and the gross morphology (bending, branching etc.) of these intact MGs did not change either. The amount of dropout and shortening was the same as before the PTPE. The excretion ducts were still intact in all samples. The MGs were cut twice in some samples, during

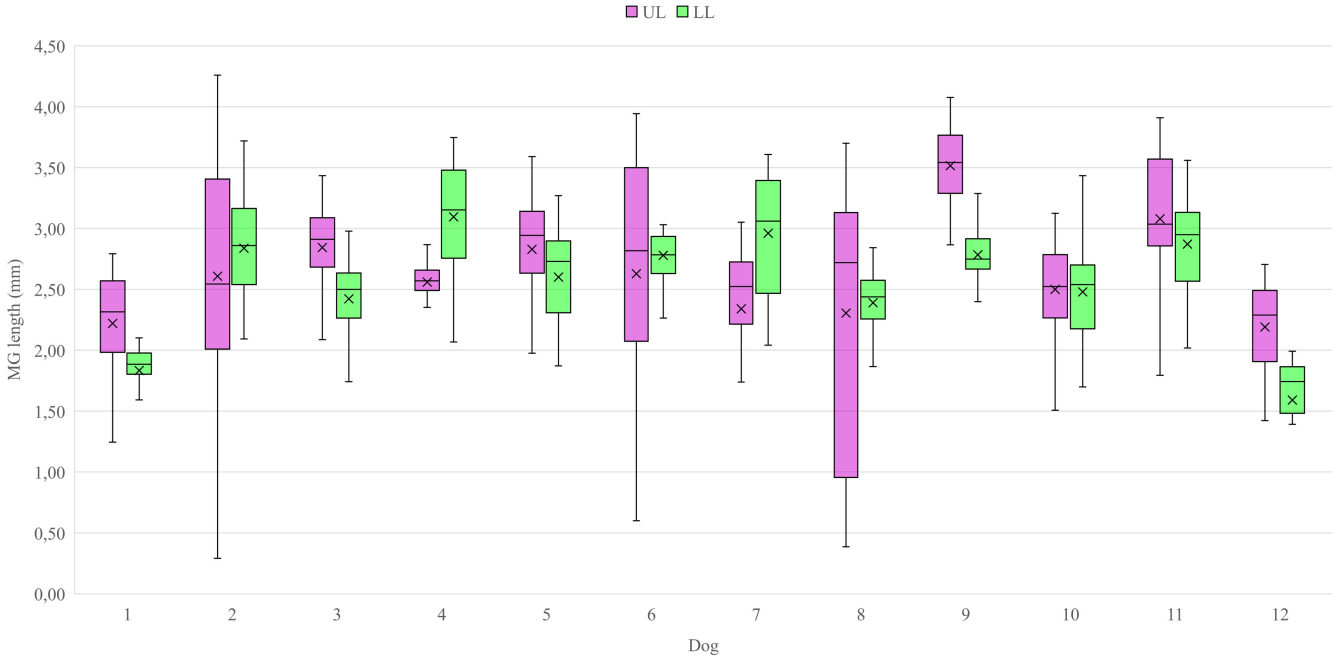

FIGURE 3 Mean, minimum and maximum of the length of individual MG in the UL and LL. LL, lower lid; MG, Meibomian gland; UL, upper lid

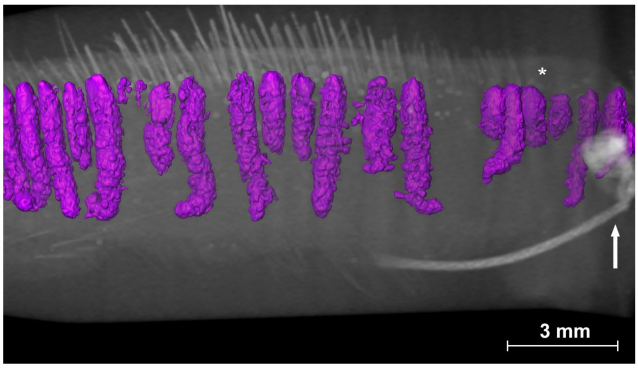

FIGURE 4 3D visualization of shortening and dropout of MGs in the UL (purple), marked with a single suture (big white arrow) of dog 6. The star (*) marks the position of the free lid margin. Isotropic voxel size = 14.8607 µm. MG, Meibomian gland; UL, upper lid

the PTPE. Both excision margins were clearly visible. No complete MGs were found in the excision. (Figure 6) After performing PTPE, remnants of the MGs of the lid margins could still be detected, in some cases even in the area of the glands further away from the free lid margin. (Figure 7) After PTPE, the average volume of the MGs in the excision was 3.09 mm^3 in the UL and 3.67 mm^3 in the LL. In the excision tissue, an average of 17.8 parts and 20.1 parts of MGs were found in the UL and LL, respectively. The volume of the MGs in the excision and the remaining lid was summed up. The total volume of MG tissue after PTPE was 12.84 mm^3 in the UL and 11.25 mm^3 in the LL. The volume of MG tissue after PTPE was positivity correlated with the volume of the MG tissue pre-PTPE; however, this value was not significant (p-value > .05).

3.3 | Results of the second scan after cryotherapy in dog 11

After cryotherapy, the area and number of MGs remained unchanged. The average length of the individual MGs decreased, from 3.08 mm precryotherapy to 2.98 mm in the UL and from 2.87 to 2.71 mm in the LL postcryotherapy. The overall morphology of the MGs and of the excretion ducts stayed the same. There was still the same Grade 1 of shortening and no dropout in the UL and LL. The volume of MGs in the upper eyelid was reduced from 29.78 mm^3 pre-cryotherapy to 28.91 mm^3 post-treatment and in the lower eyelid from 22.87 to 22.4 mm^3.

3.4 | Results of the second scan after laser therapy in dog 12

The number of MGs in the lids remained unchanged both pre and postlaser therapy. The average length of the individual MGs decreased after the procedure from 2.19 to 1.92 mm in the UL, and from 1.59 to 1.45 mm in the LL. The general morphology of the MGs did not change. However, there were changes in the appearance of the MG ducts. Some of the excretion ducts appeared pushed

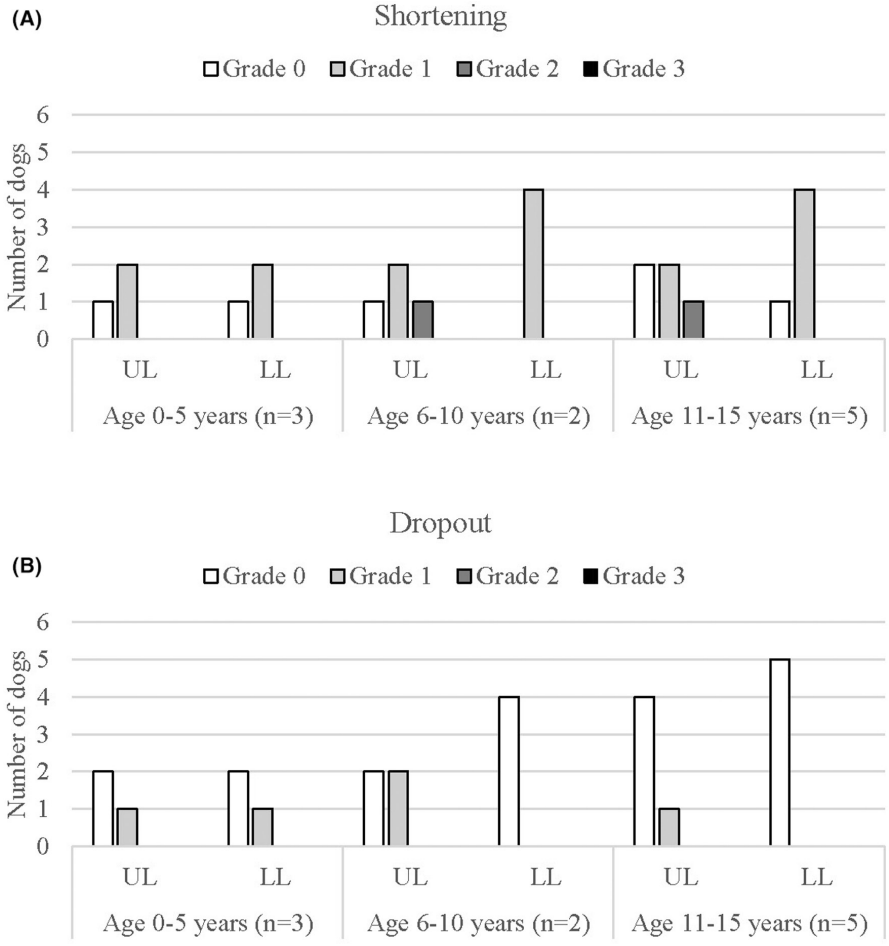

FIGURE 5 (A) Number of dogs with shortening in MGs according to different age groups. (B) Number of dogs with dropout in MGs according to different age groups. MGs, Meibomian glands

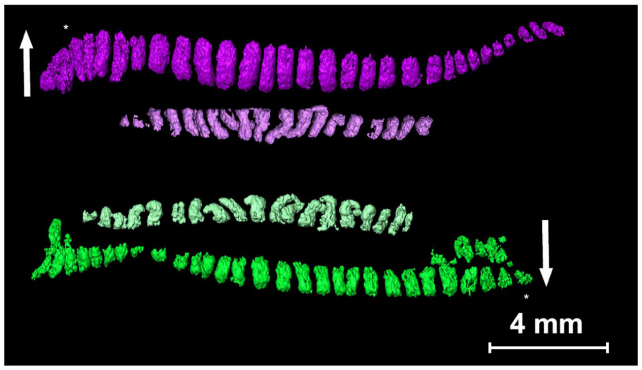

FIGURE 6 3D visualization of the UL excision (light purple) and LL excision (light green) and remaining tissue of the UL (purple) and LL (green) after PTPE in dog 1. The star (*) marks the position of the free lid margin. Isotropic voxel size = 14.8607 µm. UL, upper lid; LL, lower lid; PTPE, partial tarsal plate excision

into the MG, appearing cupped. (Figure 8) The length of the excretion ducts decreased from an average of 0.16 to 0.12 mm. The UL showed no shortening of MGs and the LL a Grade 1 shortening postlaser therapy. Both the UL and LL showed no dropout of MGs pre and postlaser therapy. The volume of MGs was 8.95 mm^3 in the UL before laser therapy and increased to 9.25 mm^3 and decreased from 6.78 to 6.38 mm^3 in the LL.

4 | DISCUSSION

4.1 | MicroCT for imaging of fresh eyelid biopsies and MGs

In this study, the morphology, number, length, and volume of MGs as well as their excretion ducts in dogs were analyzed using microCT scans.

Computed tomography (CT) is a widely established method of diagnostic imaging in veterinary medicine. CT is a cross-sectional imaging technique in which X-ray images are put together with the aid of a computer. In order to prevent falsification of the X-ray images by superimposition, several images from different angles must be taken, rotating around an axis. MicroCT provides a very high resolution, with a voxel resolution ranging from 50–1 µm.[8] During an ex vivo microCT scan, the specimen rotates around its own axis and the radiation source is stationary.[9] In vivo MicroCT has been used previously, to achieve more complex anatomic imaging of small

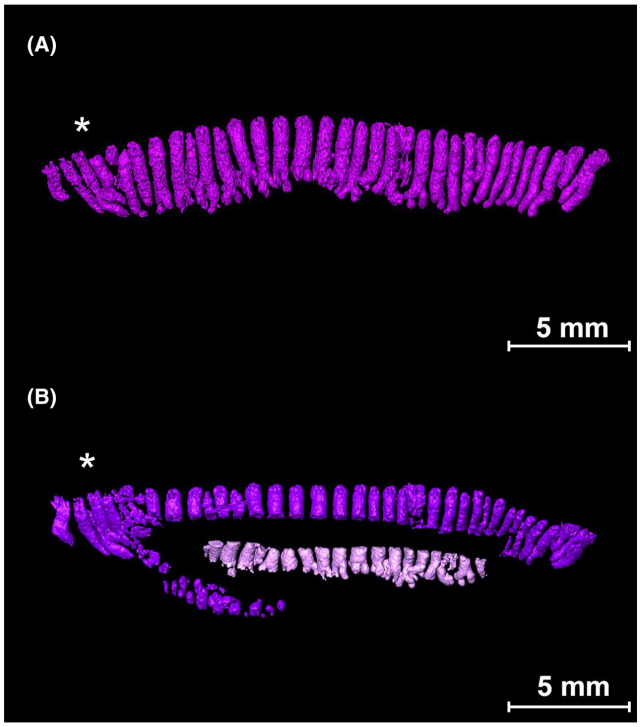

FIGURE 7 3D visualization of the UL excision (light purple) and remaining tissue of the UL (purple) before (A) and after (B) PTPE in dog 5. The star (*) marks the position of the free lid margin. Isotropic voxel size = 14.8607 μm. UL, upper lid; PTPE, partial tarsal plate excision

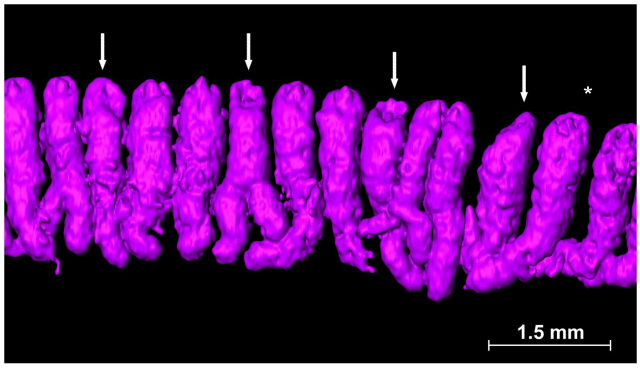

FIGURE 8 3D visualization of excretion duct cupping in the UL (purple) after lasertherapy in dog 12. The star (*) marks the position of the free lid margin. Isotropic voxel size = 14.8607 μm. UL, upper lid

animals in the monitoring of pathological processes in small animal models for human medicine.[10] However, microCT has been previously described in the literature for the visualization of vascular structure using different contrast agents, as well as for cardiac imaging, imaging of abdominal organs, the kidney, the gastrointestinal tract, liver imaging, fat quantification, and cerebral structures.[10,11] MicroCT imaging of soft tissue biopsies is possible as well, but due to the inherently low X-ray contrast of unmineralized tissues usually involves the use of X-ray dense contrast agents in order to enhance tissue contrast.[12]

There are different examples of visualization of glandular tissue using in vivo microCT. In analyzing different contrast agents for longitudinal liver and spleen microCT imaging of liver metastasis mouse models, Boll et al.[13] found contrast enhancing in the adrenal gland using a single injection of ExiTron nano and multiple injections of Fenestra LC. Additionally, Descamps et al.[14] described a good differentiation of glandular tissue using a phosphomolybdic acid (PMA) staining. Ezure et al.[15] studied abdominal skin sweat glands using microCT visualization. They were able to construct 3D images of fresh tissue biopsies without using any staining of the tissue. In an insect anatomy study, glandular tissue was visualized by the authors.[16] Gabner et al.[17] proved the existence of glandulae labiales and buccales ventrales of the dogs using microCT. Not only was it possible to visualize the small salivary glands in dogs, but it was also possible to calculate the volume as well as the length of the excretory ducts. For this study, the specimens were fixated in formaldehyde and then embedded in paraffin; one specimen was contrast enhanced, with a 1% (w/v) elemental iodine in ethanol stain.

In the present study, we chose to image fresh tissue biopsies (no fixation and no staining) in order to avoid shrinkage artifacts and to preserve the in vivo morphology of MGs. The fresh ULs and LLs were embedded in agarose. Image contrast results from the fatty meibum, which yields a lower X-ray attenuation in glandular tissue compared with adjacent tissues.

4.2 | Morphology and arrangement of MGs, and effects of PTPE, cryotherapy, and laser therapy

In this study, the length, of the area in which MGs were found, was 1.90–2.64 mm and it was not correlated to the weight of the dogs. To the authors' knowledge, there are no comparable numbers found in the literature.

A minimum of 26 and a maximum of 35 glands in the UL and LL, respectively, were counted in this study. Murphy et al.[18] report 20 to 40 glands per lid. Lawson[19] reports 20 to 25 MG openings per lid margin. Both authors do not provide specific information about breed or age of these dogs.

The MGs generally showed a parallel arrangement to the tarsal plate and to each other, close to the free lid margin. Moving further away from the free lid margin the ends of all MGs showed bending, some crisscrossing as

well as some branching, which has not been previously described in the literature.

To our knowledge, this is also the first attempt to individually measure MGs and the MG duct with microCT. Jester et al.[20] examined MGs histologically, stating a squamous epithelium lined duct, followed by numerous holocrine acini, centered around a central duct in columns. The description of columns is in line with the findings of this study. We observed changes in the length of the individual MGs. These changes have been previously described in the literature as shortening and dropout of MGs in humans.[7] This dropout has been observed both in dogs with ocular disease and in dogs without ocular disease.[21] MG deficits in a 14-year-old Cairn terrier were first diagnosed with the help of meibography and pathohistology. On pathohistology, only remnants of glandular tissue close to the excretory duct were found. These changes were classified as atrophy of the MGs due to chronic inflammation as proliferation of fibroblasts with infiltrates of plasma cells and lymphocytes. MicroCT failed to visualize any change in the tissue at the site of the absent MGs.[21] Kitamura et al.[22] demonstrate a higher number of MG dropout rates in dogs suffering from KCS and in older dogs than in young, healthy dogs. These results were only partially congruent with the results found in this study. In the present study, only one (dog 5) of 12 dogs had KCS during the time of enucleation or before enucleation. The regression model for the influence of age on the dropout of MGs was small but negative, suggesting the opposite effect of age on the probability of dropout of MGs to Kitamura et al.'s[22] statement. However, all of these calculations have to be regarded with caution due to the small sample size of both studies.

The volume of the MGs was calculated. No significant correlation to volume, age, and weight of the dog could be demonstrated.

The volumes were calculated before and after treatment with PTPE, cryotherapy, and laser therapy. After adding up the volume of the MGs in the excision and the remaining lid tissue, the total volume of the MGs was found to be lower after treatment with PTPE than before. We suspect a leakage of the meibum due to the manipulation of the eyelid margins as a reason. During PTPE, leakage of meibum from the glandular openings as well as from the excision margins themselves was observed. We assume that in microCT not the glandular tissue of the MG but rather meibum, a lipid-rich secretion, inside the MGs was visualized.

After performing PTPE, remnants of the MGs of the lid margins could still be detected in five cases (Dog 4, 5, 7, 8, and 10) even in the area of the glands further away from the free lid margin. This finding leads to the assumption that despite the PTPE, follicles of the distichia could remain in the tarsal plate. This phenomenon was also seen in the study of Palella Gomez et al.[23] A sample of 17 dogs, suffering from distichiasis, were treated with PTPE and the tarsoconjunctival specimen histopathologically analyzed. In 31 of 52 tarsoconjunctival specimen, hair follicles and/or hair shafts were identified. However, only one of the 21 eyelids, of which no follicles were found in the tarsoconjunctival excision, had recurrence. The authors suggested that in these cases the hair follicles of the distichia were not located in the MGs but rather in the Moll or Zeiss glands.[23] According to our study, the proximal part of the gland will sometimes be left in the tarsal plate even after PTPE. To avoid missing any hair follicles using PTPE, the size of the excision might have to be increased. However, caution should be taken as to not create an unwanted, cicatricial entropion.

Postcryotherapy, a slight reduction in volume of MGs was noted. We suggest that these changes are also due to manipulation of the specimen, explaining why the reduction in volume after cryotherapy and laser therapy was not as drastic as it was after PTPE. In case of laser therapy, the appearance of MG ducts may change. After laser therapy, MGs showed what we described as cupping of the gland ducts. This must be considered when using the laser therapy device. As cryotherapy and laser therapy were only done on one UL and LL each, these changes need to be interpreted carefully.

The main limitation of this study is the small sample size. Additionally, the fact that the data were collected from ex vivo lids has to be considered. To make proper associations between the influences of the treatment of distichiasis on the function of MGs, further studies have to be conducted on both healthy and affected dogs. In conclusion, we showed that microCT is an appropriate tool to visualize MGs and MG ducts, even in fresh tissue biopsies without elaborate preparation or staining. The size of MG area, the size of individual MGs, the size and shape of the MG ducts and the volume of MGs of healthy dogs pre and postdifferent distichiasis treatment options ex vivo are reported for the first time. In further studies, it should be assessed whether the function of the remaining MGs is compromised in such a level, after PTPE, cryotherapy, and laser therapy that it is clinically relevant.

CONFLICT OF INTEREST

The authors report no conflict of interest.

ORCID

Victoria Zwiauer-Wolfbeisser https://orcid.org/0000-0002-3503-998X

REFERENCES

1. Eftimov P, Yokoi N, Tonchev V, Nencheva Y, Georgiev GA. Surface properties and exponential stress relaxations of mammalian meibum films. *Eur Biophys J*. 2017;46(2):129-140.

2. Bedford PGC. Distichiasis and its treatment by the method of partial tarsal plate excision. *J Small Anim Pract*. 1973;14:1-6.
3. Raymond-Letron I, Bourges-Abella N, Rousseau T, Douet JY, De Geyer G, Regnier A. Histopathologic features of canine distichiasis. *Vet Ophthalmol*. 2012;15(2):92-97.
4. Bedford PGC. Conditions of the eyelids in the dog. *J Small Anim Pract*. 1988;29(7):416-428.
5. Scheie HG, Albert DM. Distichiasis and trichiasis: origin and management. *Am J Ophthalmol*. 1966;61(4):718-720.
6. Long RD. Treatment of distichiasis by conjunctival resection. *J Small Anim Pract*. 1991;32(3):146-148.
7. Arita R, Itoh K, Inoue K, Amano S. Noncontact infrared meibography to document age-related changes of the MGs in a normal population. *Ophthalmology*. 2008;115(5):911-915.
8. Schladitz K. Quantitative micro-CT. *J Microsc*. 2011;243(2):111-117.
9. Ritman EL. Current status of developments and applications of micro-CT. *Annu Rev Biomed Eng*. 2011;13:531-552.
10. Schambach SJ, Bag S, Schilling L, Groden C, Brockmann MA. Application of micro-CT in small animal imaging. *Methods*. 2010;50(1):2-13.
11. Boll H, Nittka S, Doyon F, et al. Micro-CT based experimental liver imaging using a nanoparticulate contrast agent: a longitudinal study in mice. *PloS One*. 2011;6(9):e25692.
12. Metscher BD. microCT for comparative morphology: simple staining methods allow high-contrast 3D imaging of diverse non-mineralized animal tissues. *BMC Physiol*. 2009;9(1):1-14.
13. Boll H, Figueiredo G, Fiebig T, et al. Comparison of fenestra LC, ExiTron nano 6000, and ExiTron nano 12000 for micro-CT imaging of liver and spleen in mice. *Acad Radiol*. 2013;20(9):1137-1143.
14. Descamps E, Sochacka A, De Kegel B, Van Loo D, Van Hoorebeke L, Adriaens D. Soft tissue discrimination with contrast agents using micro-CT scanning. *Belg J Zool*. 2014;144(1):20-40.
15. Ezure T, Amano S, Matsuzak K. Aging-related shift of eccrine sweat glands toward the skin surface due to tangling and rotation of the secretory ducts revealed by digital 3D skin reconstruction. *Skin Res Technol*. 2021;27(4):569-575.
16. Alba-Tercedor J, Hunter WB, Alba-Alejandre I. Using micro-computed tomography to reveal the anatomy of adult Diaphorina citri Kuwayama (Insecta: Hemiptera, Liviidae) and how it pierces and feeds within a citrus leaf. *Sci Rep*. 2021;11(1):1-30.
17. Gabner S, Michels C, Lanz B, Nell B, Handschuh S, Egerbacher M. Labial and buccal minor salivary glands of the dog – location, three-dimensional arrangement and histology. *Vet Ophthalmol*. 2021;24(4):400-407.
18. Murphy CJ, Samuelson DA, Pollock RVH, Evans HE, De Lahunta A. The eye. *Miller's Anatomy of the Dog*. Elsevier Saunders; 2012:767.
19. Lawson DD. Canine distichiasis. *J Small Anim Pract*. 1973;14(8):469-478.
20. Jester JV, Nicolaides N, Smith RE. Meibomian gland studies: histologic and ultrastructural investigations. *Invest Ophthalmol Vis Sci*. 1981;20(4):537-547.
21. Kitamura Y, Arita R, Miwa Y, Iwashita H, Saito A. Histopathologic changes associated with meibomian gland dropout in a dog. *Vet Ophthalmol*. 2020;23(3):575-578.
22. Kitamura Y, Maehara S, Nakade T, et al. Assessment of meibomian gland morphology by noncontact infrared meibography in Shih tzu dogs with or without keratoconjunctivitis sicca. *Vet Ophthalmol*. 2019;22(6):744-750.
23. Palella Gómez A, Mazzucchelli S, Scurrell E, Smith K, Pinheiro De Lacerda R. Evaluation of partial tarsal plate excision using a transconjunctival approach for the treatment of distichiasis in dogs. *J Small Anim Pract*. 2020;23(3):506-514.

How to cite this article: Zwiauer-Wolfbeisser V, Handschuh S, Tichy A, Nell B. Morphology and volume of Meibomian glands ex vivo pre and post partial tarsal plate excision, cryotherapy and laser therapy in the dog using microCT. *Vet Ophthalmol*. 2023;26:98-108. doi:10.1111/vop.13057